THz-range generation frequency growth in semiconductor superlattice coupled to external high-quality resonator

Vladimir V. Makarov[a,b], Vladimir A. Maksimenko[a,b], Marina V. Khramova[c],
Alexey N. Pavlov[a,d] and Alexander E. Hramov[a,b]

[a]REC "Nonlinear Dynamics of Complex Systems", Saratov State Technical University,
Politechnicheskaya Str. 77, Saratov, 410056, Russia
[b]School of Electrical and Mechanical Engineering, Saratov State Technical University,
Politechnicheskaya Str. 77, Saratov, 410056, Russia
[c]Faculty of Computer Sciences and Information Technologies, Saratov State University,
Astrakhanskaya Str. 83, Saratov, 410012, Russia
[d]Physics Dept., Saratov State University, Astrakhanskaya Str. 83, Saratov, 410012, Russia

ABSTRACT

We investigate effects of a linear resonator on spatial electron dynamics in semiconductor superlattice. We have shown that coupling the external resonant system to superlattice leads to occurrence of the additional area of negative differential conductance on the current-voltage characteristic, which does not occur in autonomous system. Furthermore, this region shows great increase of generation frequency, that contains practical interest.

Keywords: semiconductor, superlattice, high harmonics, THz, magnetic field, space charge domains, current oscillations

1. INTRODUCTION

The development of semiconductor devices working in sub-THz and THz range is now of the great interest. Such technologies are critically important for a wide range of applications[1] as astrophysics, medicine[2] and security.[3,4] Consequently, one of the most challenging tasks of modern electronics is the elaboration of the technically available sub-millimeter wavelength devices operating at room temperature.[5] Typically, the using of nano- and microstructure-based setups as quantum-cascade lasers (QCLs), transferred electron devices (TEDs) and other devices that exhibit negative differential conductance is the well-known approach in studies considering this issue.[6–8] Nevertheless, characteristics of such devices are strongly limited by it's physical dimensions such as minimal length of active media in TEDs, from which the frequency of oscillations is strongly depends.

The external resonant systems is a well-known instrument for optimization and tuning the generation characteristics of a various devices, as semiconductor active media and vacuum electronics as BWO. Moreover, external resonant systems also can be utilized to obtain the different dynamical regimes, as chaos and quasi-periodicity.

One of the promising devices demonstrating spectrum containing powerful harmonics and working in sub-THz range is the semiconductor superlattice (SL). Semiconductor superlattices are composed from alternating layers of different semiconductor materials (two or more) with different band width. Such periodic structure promotes the formation of minibands in which electrons can travel along the semiconductor superlattice. If the product of the carrier concentration within the device and the sample length exceeds a critical value, the NDC triggers the formation of propagating charge domains, which could be utilized both for generation and amplification of sub-THz/THz radiation.[9–11]

Recently, we have shown the possibility to obtain the chaotic oscillations in the semiconductor superlattice coupled to external quality resonator.[12–14] In this report we study numerically the effect of external resonator on the current-voltage characteristic of SL. We show the appearance of the additional NDC region, that is caused by high-frequent field oscillations in external quality resonator.
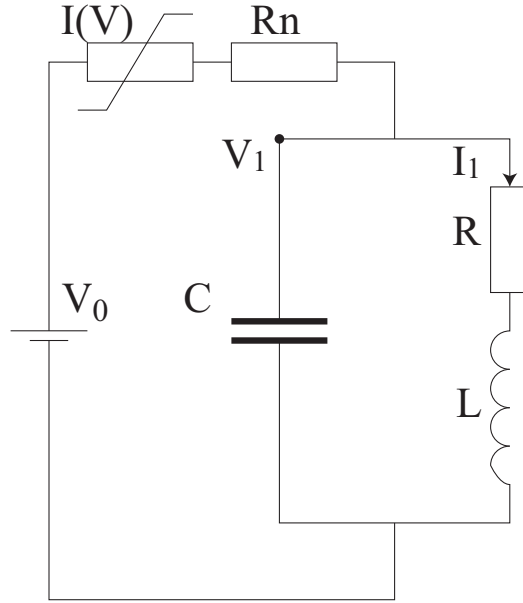
Figure 1. Equivalent scheme of SL coupled to external resonant circuit. V_0 denotes the supply voltage, $I(V_s l)$ and $V_s l$ is the current flowing through the SL and the voltage drop on the SL contacts, respectively.

2. NUMERICAL MODEL

To investigate the collective electron transport in superlattice we use the model described in,[14–16] with the semiconductor superlattice parameters taken from recent experiments.[13] The miniband transport region is discretized into $N = 480$ layers, each of width $\delta x = 0.24$ nm, small enough to approximate a continuum and ensure convergence of the numerical scheme. The discretized current continuity equation is

$$e\delta x \frac{dn_m}{dt} = J_{m-1} - J_m, \qquad m = 1 \ldots N, \tag{1}$$

where $e > 0$ is the electron charge , n_m is the charge density at the right-hand edge of mth layer, at position $x = m\delta x$, and J_{m-1} and J_m are the areal current densities at the left and right hand boundaries of the mth layer

$$J_m = en_m v_d\left(\overline{F}_m\right), \tag{2}$$

where $\overline{F}_m$ is the mean field in the mth layer.[15] The drift velocity, $v_d(\overline{F})$, corresponding to electric field, $\overline{F}$, can be calculated as in:[17]

$$v_d = \frac{\Delta d}{2\hbar} \frac{I_1(\Delta/2k_B T)}{I_0(\Delta/2k_B T)} \frac{e\overline{F}d\tau/\hbar}{1 + (e\overline{F}d\tau/\hbar)^2}, \tag{3}$$

where $d = 8.3$ nm is the period of the SL, $\Delta = 19.1$ meV is the miniband width, $T = 4.2$ K is the temperature, k_B is the Boltzmann constant and $I_n(x)$, where $n = 0, 1$, is a modified Bessel function of the first kind.

The electric fields F_m and F_{m+1} at the left- and right-hand edges of the mth layer respectively, are related by the discretized Poisson equation

$$F_{m+1} = \frac{e\delta x}{\varepsilon_0 \varepsilon_r}(n_m - n_D) + F_m, \quad m = 1 \ldots N, \tag{4}$$

where ε_0 and $\varepsilon_r = 12.5$ are, respectively, the absolute and relative permittivities and $n_D = 3 \times 10^{22}$ m^{-3} is the n-type doping density in the semiconductor superlattice layers. The current density injected into the contact layers of the semiconductor superlattice subjected to the field F_0 is $J_0 = \sigma F_0$, where $\sigma = 3788$ Sm^{-1} is the
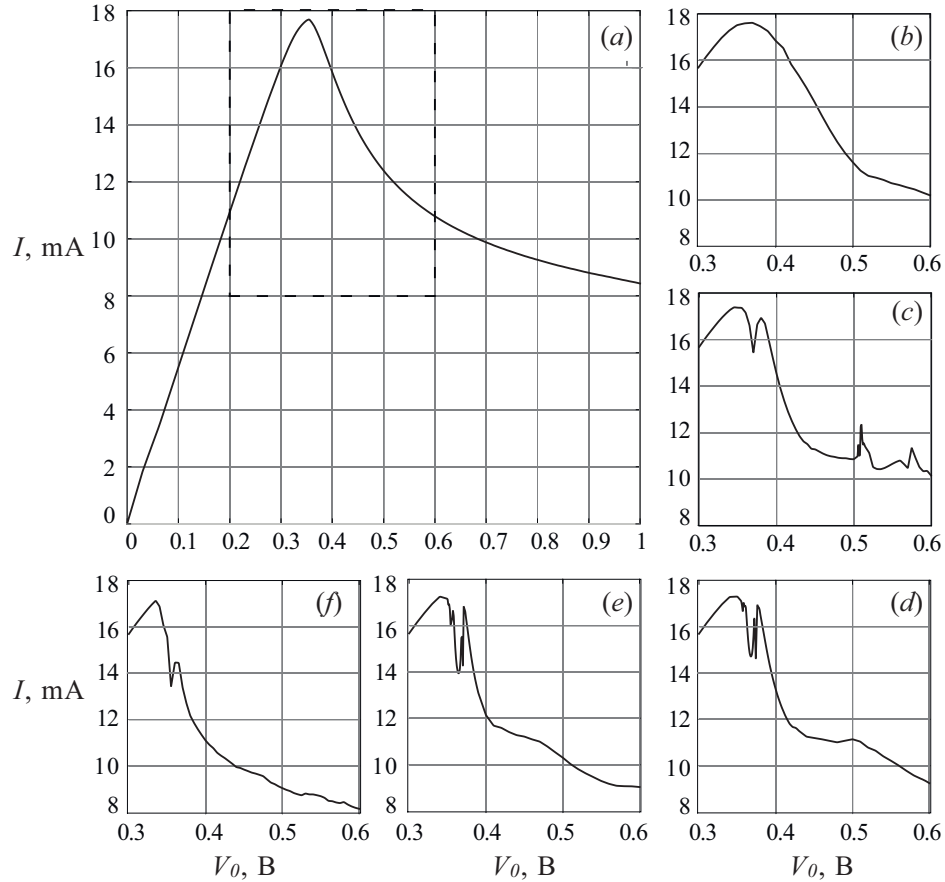
Figure 2. Current-voltage characteristics of autonomous SL (a) and SL coupled to external circuit with several resonant frequencies: (b) $f_Q = 10.04$, (c) $f_Q = 13.81$, (d) $f_Q = 15.45$, (e) $f_Q = 18.27$, (f) $f_Q = 45.10$. Quality factor $Q = 150$

conductivity of the heavily-doped emitter.[15] The voltage, V_{sl}, dropped across the semiconductor superlattice defines a global constraint:

$$V_{sl} = U + \frac{\delta x}{2} \sum_{m=1}^{N} (F_m + F_{m+1}), \tag{5}$$

where the voltage, U, dropped across the contacts includes the effect of charge accumulation and depletion in the emitter and collector regions, and the voltage across the contact resistance,[18] $R = 17\ \Omega$. The current through the device is

$$I(t) = \frac{A}{N+1} \sum_{m=0}^{N} J_m, \tag{6}$$

where $A = 5 \times 10^{-10}\ \text{m}^2$ is the cross-sectional area of the semiconductor superlattice.[15, 18]

We considering the superlattice interacting with the external resonant circuit as shown in Fig. 1 and apply the Kirchoff's equations to simulate it's dynamics in the single-mode assumption:

$$\frac{dV_1}{dt} = \frac{I(V_{sl}) - I_1}{C}, \quad \frac{dI_1}{dt} = \frac{V_0 - V_{sl} + RI_1 + R_l I(V_{sl})}{L}, \tag{7}$$

where $V_1(t)$ and $I_1(t)$ are, respectively, the voltage across the capacitor and the current through the inductor. Thus, the voltage dropped across the SL is $V_{sl} = V_0 - V_1 + V_e xt cos(\omega_{ext}t)$, where $V_e xt$ and ω_{ext} is the amplitude and frequency of external informational signal respectively. The eigenfrequency of the resonator is $f_Q = 1/(2\pi\sqrt{LC})$ and the quality factor is $Q = (1/R)\sqrt{L/C}$.
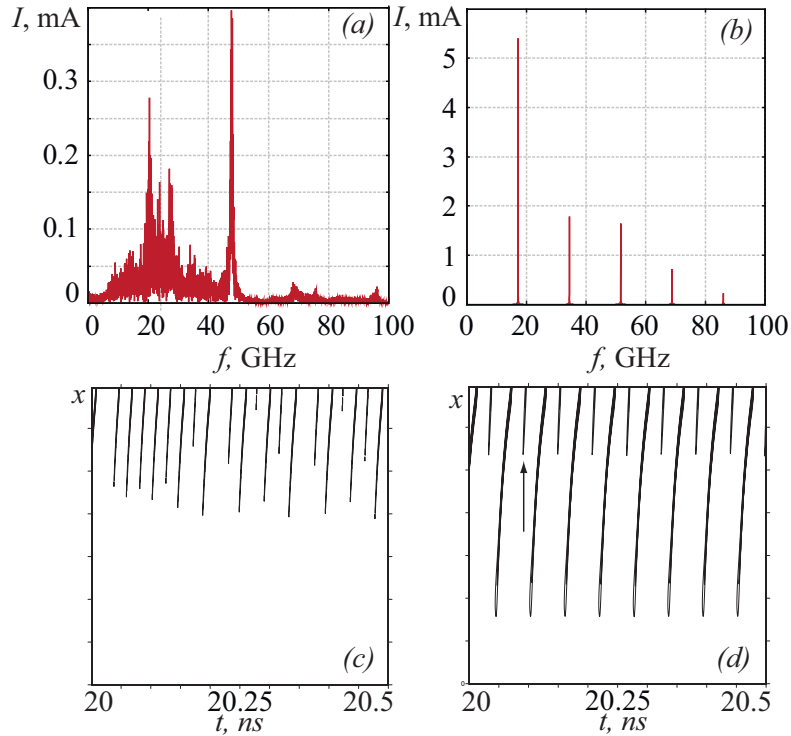
Figure 3. Amplitude spectrums (a, b) and spatio-temporal distributions of charge in the transport region of SL (c, d) for different supply voltage: 340 mV (a, c), 350 mV (b, d). The resonant frequency of external circuit $f_Q = 104.5$ GHz, quality factor $Q = 150$.

3. SIMULATIONS

To study the effect of resonator on current dynamics in the SL we have compared the IV-characteristic of autonomous system with characteristics, calculated for various frequencies of external resonator, that are presented in Fig. 2. The current-voltage characteristic for the autonomous case (Fig. 2 (a)) present itself the typical Esaki-Tsu curve, that exhibit one maxima, that marks the beginning of NDC region. In this case SL demonstrates only periodic current oscillations, that denotes the main frequency of generation.

The Fig. 2 (b-f) shows the region near the Esaki-Tsu peak, that is marked in figure (a) by the dashed square, for the SL coupled to resonator with different frequencies. The case (b) corresponds to $f_Q = 10.04$ GHz. The small deformation of the characteristic can be observed, but, no additional extremes appears. If we increase the eigenfrequency of resonator up to $f_Q = 13.81$ (Fig. 2(c)), several additional peaks arise on curve. The maxima in the region 0.5-0.6 mV are corresponding to the transitions between dynamical regimes,[13] while the irregularity at ≈ 0.35 mV present itself the additional region of negative differential conductance. The further increase of resonator frequency results in disappearance of irregularities at 0.5-0.6 mV, and small increase of additional NDC region (Figures 2 (d-f)).

To study this effect in detail the spectrums of current oscillations and the spatio-temporal distributions of charge in SL was calculated for two values of supply voltage, one of which corresponds to appeared NDC area, and the second one corresponds to the higher voltage (see Fig. 3). One can see principal difference between the realizing regimes. The regime, corresponding to the additional NDC area is characterized by the broadband spectrum, that exhibit two strongly pronounced frequencies, one of which is close to 50 GHz. Increasing of supply voltage results in transition to periodical regime, and the amplitude grows greatly. Nevertheless, the spectrum now exhibit only one fundamental frequency, $f \approx 18$ GHz, corresponding to the time of domain propagation. Although, spectrum contains the number of powerful highest harmonics.

Considering the charge dynamics in SL, we can see that both pictures demonstrate the alternation of weak domain with low charge concentration and the "stronger" domain. The transition to regime, shown in Fig 3(d) is accompanied by growth of charge concentration in the "strong" domain, that results in stabilization of system dynamics.

4. CONCLUSIONS

In this paper we report the results of the study of the effect of external resonator on current dynamics in semiconductor superlattice. We show, that coupling of external quality resonator to superlattice results in the appearance of an additional area of negative differential conductance, that is characterized by the chaotic regime and increasing of the frequency of generation. The observed effects contain practical interest for the development of new sub-THz broadband sources,[2] including the carrier generators for the data transmission systems.[19]

REFERENCES

[1] Bartalini, S., Consolino, L., Cancio, P., De Natale, P., Bartolini, P., Taschin, A., De Pas, M., Beere, H., Ritchie, D., Vitiello, M. S., and Torre, R., "Frequency-comb-assisted terahertz quantum cascade laser spectroscopy," *Phys. Rev. X* **4**, 021006 (2014).

[2] Yu, C., Fan, S., Sun, Y., and Pickwell-MacPherson, E., "The potential of terahertz imaging for cancer diagnosis: A review of investigations to date," *Quant Imaging Med Surg* **2**, 33–45 (2012).

[3] Tekavec, P.F. and Kozlov, V. G., "High power THz sources for nonlinear imaging," *AIP Conf. Proc.* **253**, 1576 (2014).

[4] Kashiwagi, T., "Computed tomography image using sub-terahertz waves generated from a high-tc superconducting intrinsic josephson junction oscillator," *Appl. Phys. Lett.* **104**, 082603 (2014).

[5] Kristinsson, K., Kyriienko, O., and Shelykh, I. A., "Terahertz laser based on dipolaritons," *Phys. Rev. A* **89**, 023836 (2014).

[6] Polyushkin, D. K., Márton, I., Rácz, P., Dombi, P., Hendry, E., and Barnes, W. L., "Mechanisms of THz generation from silver nanoparticle and nanohole arrays illuminated by 100 fs pulses of infrared light," *Phys. Rev. B* **89**, 125426 (2014).

[7] Dekorsy, T., Auer, H., Bakker, H., Roskos, H., and Kurz, H., "THz electromagnetic emission by coherent infrared-active phonons," *Phys. Rev. B* **53**, 4005–4014 (1996).

[8] Selskii, A. O., Koronovskii, A. A., Hramov, A. E., Moskalenko, O. I., Alekseev, K. N., Greenaway, M. T., Wang, F., Fromhold, T. M., Shorokhov, A. V., Khvastunov, N. N., and Balanov, A. G., "Effect of temperature on resonant electron transport through stochastic conduction channels in superlattices," *Phys. Rev. B* **84**, 235311 (2011).

[9] Gunn, J. B., "Instabilities of current in iii-v semiconductors," *IBM J. Res. Dev.* **8**, 141 (1964).

[10] Koronovskii, A. A., Maximenko, V. A., Moskalenko, O. I., Hramov, A. E., Alekseev, K. N., and Balanov, A. G., "Transition to microwave generation in semiconductor superlattice," *Physics of wave phenomena* **21**(1), 48–51 (2013).

[11] Maksimenko, V. A., Makarov, V. V., Koronovskii, A. A., Alekseev, K. N., Balanov, A. G., and Hramov, A. E., "The effect of collector doping on the high-frequency generation in strongly coupled semiconductor superlattice," *Europhysics Letters* **109**, 47007 (2015).

[12] Makarov, V. V., Hramov, A. E., Koronovskii, A. A., Alekseev, K. N., Maksimenko, V. A., Greenaway, M. T., Fromhold, T. M., Moskalenko, O. I., and Balanov, A. G., "Sub-terahertz amplification in a semiconductor superlattice with moving charge domains," *Applied physics letters* **106**, 043503 (2015).

[13] Hramov, A. E., Koronovskii, A. A., Kurkin, S. A., Makarov, V. V., Gaifullin, M. B., Alekseev, K. N., Alexeeva, N., Greenaway, M. T., Fromhold, T. M., Patane, A., Kusmartsev, F. V., Maximenko, V. A., Moskalenko, O. I., and Balanov, A. G., "Subterahertz chaos generation by coupling a superlattice to a linear resonator," *Phys.Rev.Lett.* **112**, 116603 (2014).

[14] Koronovskii, A. A., Hramov, A. E., Maximenko, V. A., Moskalenko, O. I., Alekseev, K. N., Greenaway, M. T., Fromhold, T. M., and Balanov, A. G., "Lyapunov stability of charge transport in miniband semiconductor superlattices," *Phys. Rev. B* **88**, 165304 (2013).

[15] Greenaway, M. T., Balanov, A. G., Schöll, E., and Fromhold, T. M., "Controlling and enhancing terahertz collective electron dynamics in superlattices by chaos-assisted miniband transport," *Phys. Rev. B* **80**, 205318 (2009).

[16] Maksimenko, V. A., Koronovskii, A. A., Hramov, A. E., Makarov, V. V., Moskalenko, O. I., Alekseev, K. N., and Balanov, A. G., "Model for studying collective charge transport at the ohmic contacts of a tightly coupled semiconductor nanostructure," *BRAS: Physics* **78**(12), 1285–1289 (2014).

[17] Romanov, Y., "Nonlinear effects in periodic semiconductor structures," *Optika i Spektroskopiya* **33**, 917 (1972).

[18] Wacker, A., "Semiconductor superlattices: a model system for nonlinear transport," *Physics Reports* **357**, 1–111 (2002).

[19] Materassi, D. and Basso, M., "Time scaling of chaotic systems: Application to secure communications," *Int. J. Bifurcation Chaos* **18**, 567–575 (2008).